ORIGINAL PAPER

Enhancement of Poly(vinyl chloride) Electrolyte Membrane by Its Exposure to an Atmospheric Dielectric Barrier Discharge Followed by Grafting with Polyacrylic Acid

Mohamed Abu-Saied[1] · Alaa Fahmy[2] · Nasser Morgan[3] · Walid Qutop[2] · Hassan Abdelbary[2] · Jörg Florian Friedrich[4]

Abstract

A poly(vinyl chloride) (PVC) membrane was exposed to atmospheric-pressure dielectric barrier discharge and subsequently wet-chemically grafted with poly(acrylic acid) (PAA) and then consumed with poly(ethyleneimine) (PEI). The thus modified membrane was characterized by measurement of the static water contact angle, by scanning electron microscopy, infrared spectroscopy (ATR-FTIR), thermogravimetry (TGA) and electrolytic responses. The TGA favors a thermally stable grafted PVC membrane. The ATR-FTIR revealed the existence of an ultra-thin PAA layer grafted onto the surface of the plasma-modified PVC membrane. The ion exchange capacity measurement of the grafted poly(vinyl chloride) (PVC–PAA) sample was close to that of additionally wet-chemically aminated with PEI for 12 h or more (PVC–PAA–PEI). It means that PVC–PAA membranes do not need necessarily further modifications. As concomitant helpful effect, it was observed that the swelling degree of the PVC membrane was reduced after plasma exposure due to plasma-induced crosslinking.

✉ Alaa Fahmy
alaa.fahmy@azhar.edu.eg

✉ Jörg Florian Friedrich
friedrich-erkner@t-online.de

1 Polymeric Materials Research Department, Advanced Technology and New Materials Research Institute (ATNMRI), City of Scientific Research and Technological Applications (SRTA-City), New Borg Al-Arab City, Alexandria 21934, Egypt

2 Department of Chemistry, Faculty of Science, Al-Azhar University, Cairo 11884, Egypt

3 Physics Department, Faculty of Science, Al-Azhar University, Cairo 11884, Egypt

4 Polymertechnik und Polymerphysik, Technical University Berlin, Ernst-Reuter-Platz 1, 10587 Berlin, Germany

Introduction

Polymer electrolyte membrane (PEM) based fuel cells are widespread because of their hazard-free electricity generation potential. Proton and alkaline fuel cells use PEMs as proton and hydroxyl ions conducting membranes, respectively [1, 2]. The sulfonated tetrafluoroethylene-based fluoropolymer is the most widely used PEM (ordinarily referred as Nafion). These membranes are accounted to have safely high conductivity corresponding to high concentrations of the proton exchanging groups. However, their inherent impediments, such as prohibitive cost, permeability and low activity as electro-catalysts, have greatly restricted their wide utilization in fuel cells [3, 4]. Honorable efforts were made to achieve and develop the techniques for preparing new or modified PEMs [5, 6]. Recently, plasma was considered to give great promises and it represents an advanced technique in the PEMs technology [7–9].

Plasma treatment was found to be an efficient and unique technique for grafting the surface of membranes with polymers. Such modifications occurred on the topmost surface almost unaffecting the bulk properties of the membrane. Such grafting is usually accomplished by treatment of the target membranes with plasma in argon or nitrogen or oxygen/air to generate reactive anchoring points for a following graft polymerization process [10]. As discussed by Bebin et al. [11], the hydration of the blended Laponite/Nafion membranes was improved using the plasma treatment for grafting of Laponite with p-styrene sulfonic acid. The thus modified Nafion/grafted Laponite membranes exhibited 20% amendment of power to fuel cells in comparison to the commercial Nafion. Additionally, Navarro et al. [10] have been reported that plasma modified polyethylene could improve the accessibility of membranes for applications in fuel cells.

Plasma processes performed under low-pressure conditions are well established since many decades and utilized in industry [12]. In spite of their wide advantages, low-pressure plasma stays contestable because of expensive devices, tools, conditions and small scale or limiting to batch processes. Thus, the equivalent plasma techniques at atmospheric pressure is the Dielectric Barrier Discharge (DBD), which is simple in processing and costs in comparison to the low-pressure process [13, 14].

The chemical effects of plasma exposure of polymer surfaces can be characterized by introduction of atoms and groups from the plasma gas into the polymer surface as well as branching, crosslinking, etching (increasing the surface area) as further effects. The introduction of functional groups is associated with increasing of hydrophilicity and generation of anchoring points for grafting. It is superposed by auto-oxidative post-plasma reaction of plasma-generated radicals with molecular oxygen from ambient air followed by formation of peroxide and hydroperoxide groups and their decay to various O-functional groups [15, 16]. The scope of these effects depends on the wide variation range of parameters such as power, treatment time, discharge current and used gas type. Among the different plasma processes plasma polymerization is an interesting method because the type of precursor and the variation of deposition conditions let tune some of its physicochemical properties [17, 18].

Plasma coating with poly(acrylic acid) (PAA) or poly(methyl methacrylate) (PMMA) [19] were commonly utilized in painting industry because of their good adhesion to metallic substrates [20]. Acrylic acid (AA) is a simple and very reactive monomer for deposition or grafting of thin organic films using the plasma [21, 22]. Moreover, AA can be applied for modification of the surface of biomaterials by its grafting using reactions with plasma-produced reactive sites and AA in solution [23].

It means that exposure of PVC to plasma generates radicals or double bonds by elimination of H, Cl or HCl followed by amination or sulfonation. Alternatively, pin-hole free thin films of PAA were obtained by plasma polymerization, however, without defined covalent bonding to the PVC.

The O_2 and also the air gas plasma have a strong oxidizing action. Oxygen plasma is used for removing all organic contaminants from the surface. Then, O-containing groups were incorporated into the topmost surface layer of polymers before etching begins [24, 25].

Such plasma-introduced reactive sites could initiate grafting from. Plasma introduced functional groups can also be used as anchoring points for covalent bonding of monomers with reactive groups by reaction of functional groups. Here, plasma was used to generate radicals which can start the before mentioned graft polymerization with reactive vinyl, acrylic or diene monomers [26]. Three principal routes are possible: (a) direct consumption of substrate radicals with the reactive monomer and thus starting a graft copolymerization from, (b) it is more easy to consume the C radicals with oxygen from air, thus forming peroxy groups, followed by formation of hydroperoxides and finally decomposition of hydroperoxides into radical species which can also start a "graft-copolymerization from", Thus, covalent C–O–C or C–O–O–C bonds hold the growing graft chain, (c) ordinary chemical reactions take place between the plasma-introduced functional groups at the surface of the substrate and functional groups of the graft molecule by "grafting to" via nucleophilic substitution.

Perni et al. [27] discussed the role of cold atmospheric He–O_2 plasma treatment on polyethylene (PE) while D'Sa et al. [28] reported the influence of the DBD plasma treatment of polymers in air atmosphere on cell response and adhesion of proteins. Additionally, Shao et al. [29] also studied the improvement of surfaces and adhesion properties of polyimide by exposure to the air DBD with filamentary and homogeneous plasma. O-containing groups are important in biomedical and fuel cells applications. The diverse O-functional groups can assist and improve also the adhesion and therefore they are used for biomolecule immobilization [30].

The general effect of all plasma treatments is the change of hydrophobic polymer surfaces to hydrophilic ones. This effect would be considered as most essential for technical use of electrolytic membranes made of poly(vinyl chloride) (PVC). Therefore, this work focuses on the grafting of acrylic acid onto plasma-activated poly(vinyl chloride) membrane surfaces. The introduced COOH groups promise the generation of an exceptional strong hydrophilic surface.

Additionally, the sensitivity of carboxylic groups to pH changes in solutions, in which they are immersed, plays a significant role for example in drug delivery application. One of the major challenges in drug applications is ensuring that the candidate is delivered to the right place which depending on the pH values. Therefore, it can be used in drug delivery systems to release the active ingredient in the desired amount at the correct place in intestine which is characterized by a specific pH [31].

Moreover, the thermal stability of the modified membranes was evaluated compared to the blank one by thermogravimetric analysis. The effect of additional amination of the PAA-grafted PVC membrane with polyethyleneimine and ethylenediamine was examined in detail. The stability of grafted films in water was investigated, too. Finally, ion exchange capacity measurements were utilized to characterize the ability of suspended material to undergo transport of ions.

Experimental

Materials

Acrylic acid (AA) 99%, poly(vinyl chloride) (PVC) with $M_W \sim 48,000$ g/mol as fine powder, tetrahydrofuran (THF, 99.5%) and poly(ethyleneimine) with 99% purity were purchased from Sigma-Aldrich chemicals company, Germany, Belami Fine Chemicals co., Mumbai, India, Fisher chemicals co. and Across for chemicals company, respectively. Figure 1 presents the chemical structures of used substances.

Preparation of the Membrane

PVC membranes were produced by casting of PVC solutions of THF (3 wt%) between glass plates utilizing a spreader knife. The solvent was evaporated completely after 24 h at 60 °C. The measured thickness of the membranes was in the range from 0.04 to 0.08 mm. The thickness of the ultra-thin layers of grafted PAA deposited onto PVC was ~ 2.5 nm. To calculate the thickness of the ultra-thin film, the density of 1 g cm^{-3} was assumed for the deposition onto a quartz-microbalance. The calculated thicknesses may have an error ($\pm 10\%$); however, this error value was the same in all the cases and therefore, the relative changes can be discussed.

Plasma Processing

The DBD equipment ignites the electrical discharge between two metal electrodes. The powered electrode was isolated by a dielectric as presented in Fig. 2.

The discharge cell includes two circular stainless-steel electrodes of 15 cm in diameter, separated by a Pyrex glass sheet through an O ring leaving a gap space of about 1 mm. The grounded metal electrode was fixed on a Perspex sheet through fixing nails which were connected to the ground through a 100 Ω resistance. The powered electrode was connected to a high voltage setup transformer which generates a sinusoidal voltage (50 Hz, 0–12 kV, 30 mA) to drive the discharge. The working gas was injected to the discharge zone through holes in the grounded electrode. A limiting resistor connected between the power supply and powered electrode R_L was used for controlling the discharge current, stabilizing the discharge and preventing the formation of a spark discharge.

The polymer foils were inserted into the discharge gap between two electrodes and treated for 10 min. The current and the voltage waveforms were detected with 100 MHz with a two-channel digital storage oscilloscope (Type HM1508); one of them was jointed to a high voltage potential divider (1:1000) to record the voltage. The other channel was attached to a 100 Ω resistance connected between the ground and the
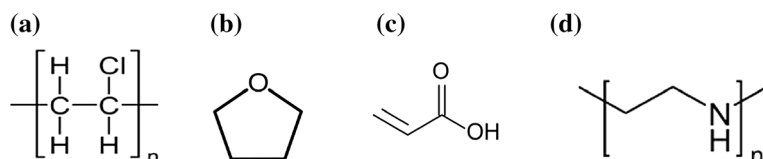

Fig. 1 Representation of chemical structures **a** PVC, **b** THF, **c** acrylic acid, **d** polyethyleneimine
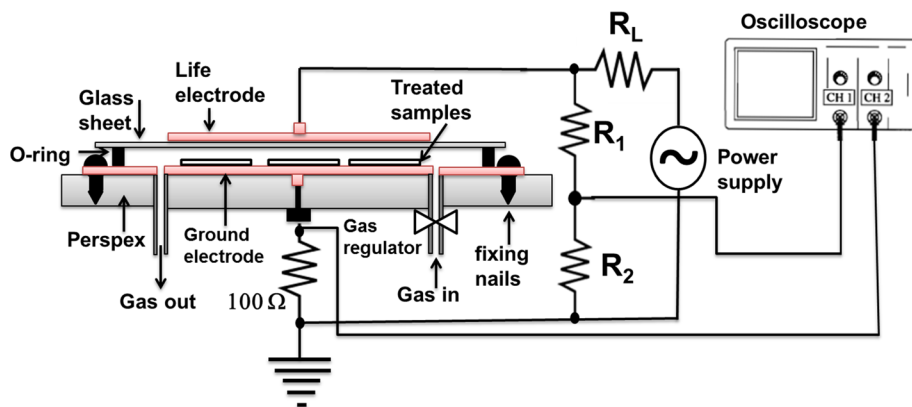
Fig. 2 Schematic diagram of the planar DBD

grounded electrode to detect the current of the discharge. The consumed power was investigated by substituting the 100 Ω resistance with a 10 nF capacitor to calculate the charge accumulated in the discharge cell. The discharge power was measured using the Q–V Lissajous figure following the method of Manley [32, 33].

After finishing the plasma treatment process in oxygen environment, the PVC membrane was directly dipped into 10 mL of liquid acrylic acid monomer (AA) for 1 h (grafting process), then washed with water. Subsequently, the primary grafting process was followed by a second grafting process, the chemical consumption of carboxylic groups with amines (amination) by immersing the grafted sample in 10 mL of 10% poly(ethyleneimine) for 18 h, then laundered with deionized water again and dried for 1 h at 60 °C in a vacuum oven.

Instrumental Characterizations

Contact Angle Measurements

A contact angle goniometer VCA 2500 XE equipped with a CCD camera and analysis software (AST Products, Billerica, MA) were utilized to measure each 5 times the static contact angle of a water droplet deposited onto the prepared membrane as an indicator for its hydrophilicity [34]. The dissolution of Low-Molecular Weight Oxidized Material, produced by the plasma exposure, into the water drop was not considered.

Characterization by FTIR

The chemical structure and the interaction with the (grafted) polymer on the membranes were characterized via Fourier transform infrared spectrometer (FTIR) (Shimadzu FTIR-8400s, Japan) using the attenuated total reflectance (ATR) mode with a diamond crystal. The spectra were scanned in the range of wavenumbers from 400 to 4000 cm^{-1}.

SEM Topography

The morphological features and the microstructure of the PVC membranes were documented by scanning electron microscopy (SEM) using a JEOL JSM-6360LA microscope, Japan. Sample scanning operated at an acceleration voltage of 20 kV. The membranes were pasted onto stainless steel stubs with double tape, and then a layer of gold was sputtered with a thickness of 10–20 nm using the sputtering device from JEOL Ltd., Tokyo, Japan. Magnifications varied from 500 to 20,000 [35].

Thermogravimetric Analysis (TGA)

Thermogravimetric analysis was utilized to discuss the thermal stability of the resultant polymer composite membrane through measuring weight loss with increasing the temperature gradually at a constant heating rate. Therefore, thermogravimetric analysis was performed by a Shimadzu TGA-50 in the range from ambient temperature to 800 °C with a 10 °C/min heating rate [36].

Mechanical Properties of the Membrane

The tensile strength of the membranes was investigated using the Universal Testing Machine (Shimadzu UTM, Japan). Measurements were performed at room temperature. The specimens were 30×10 mm and measurements carried out at constant speed of cross heads of 5 mm/min [37]. At least three measurements were done for each sample and the mean values were taken for discussion.

Ion Exchange Capacity (IEC)

IEC is generally determined by using a volumetric probe based on the measurement of functional groups existing in the polymer membrane. A membrane sample in the H^+ counter ion form was drenched in 20 mL of 2 molar NaCl solution at room temperature for 12 h and then the concentration of HCl freed from the membrane was titrated with a standard solution of 0.1 N NaOH in presence of phenolphthalein as indicator. IEC in mills equal to the functional groups per gram of dry sample was recorded as shown in Eq. (1) [38]:

$$IEC = \text{Titrate value (mL)} \cdot \text{Normality of NaCl/Wt of dry polymer membrane (g)}$$

(1)

Uptake of Liquids

The water, methanol and ethanol uptake of the treated and grafted PVC was measured in comparison to the untreated membranes. For analyzing the swelling efficiency of PVC-g-PAA graft membranes, the samples were cut into square form with length = 2 cm and dried in vacuum oven for 12 h and then weighted (W_{dry}). The dried samples were immersed in deionized water, methanol and ethanol at room temperature, then the sample were weighted (W_{wet}) for each solvent at specific interval times. The water uptake of the testers was given as [1]:

$$\text{uptake (\%)} = \left[\left(W_{wet} - W_{dry} \right) / W_{dry} \right] \times 100$$

Results and Discussion

Description of Electrical Properties

Current–Voltage Waveform

The current–voltage oscillogram of the coaxial DBD system, recorded at atmospheric pressure and room temperature, is presented in Fig. 3. The measured current is composed of three components, displacement current, filamentary current and glow current. The displacement current is the current passing through the cell when the applied voltage is unable to ignite the plasma. The filamentary and glow current are two common modes of discharge current in DBD when the applied voltage exceeds the breakdown voltage.

To understand the electrical properties of the DBD a simple electrical equivalent circuit represent the DBD operation is shown in Fig. 4. In the non-ignited case (key in position 1) the equivalent circuit is purely capacitive and consists of two capacitances, one is resembling the dielectric barrier capacitance C_d and the other is the gas gap capacitance C_g. The sum of the voltages across the gas gap V_g and the barrier V_d equals to the applied voltage $V(t)$. When the voltage V_g is too low to cause discharge ignition as long as the amplitude of the applied voltage is below a certain threshold V_{min} and the current is only the capacitive displacement current $I_{displacement}$ as shown in Fig. 3 (Eq. 2).

$$I_{displacement}(t) = (C_D C_g / C_D + C_g) \frac{dV(t)}{dt} \qquad (2)$$

The discharge ignited (key in position 2) when the applied voltage magnitude exceeds the threshold V_{min} (breakdown voltage) at which the instantaneous gap voltage reaches a certain threshold, which is determined by the gas composition, its pressure and the discharge gap. Additional current is formed which is the discharge current (glow and filamentary current) shown in Fig. 3. In this case more charge (Q) is transferred into the gap.
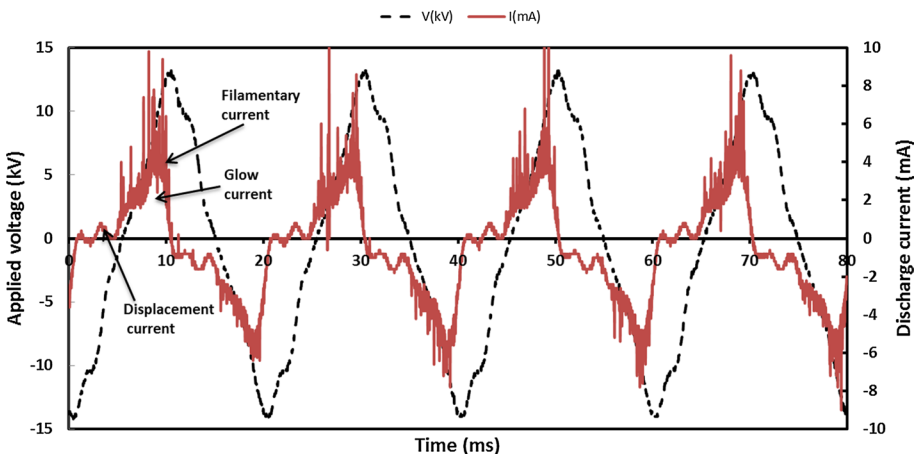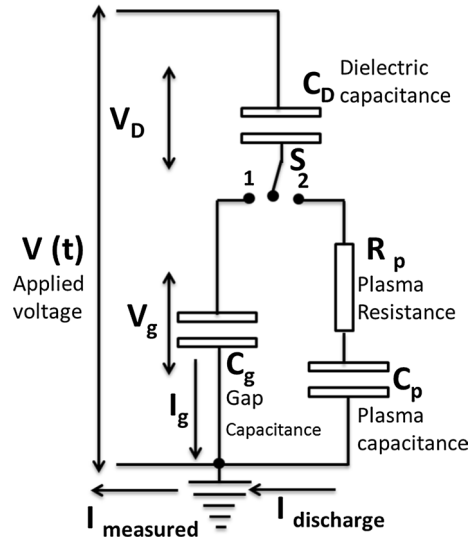

Fig. 3 Current–voltage oscillogram at an applied voltage of 14 kV

Fig. 4 Electrical model of DBD discharge operation

The relation between the gap voltage $V_g(t)$ and the total charge Q(t) are written as follows [39] (Eq. 3):

$$Q(t) = \left(1 - \frac{C_{cell}}{C_d}\right)Q_{disg}(t) + C_{cell}V(t)$$

$$C_{cell} = \frac{C_g C_d}{C_g + C_d}$$

(3)

Q_{disg} is the charge which is transferred conductively during the discharge, C_{cell} is the total capacitance of the discharge cell including both the dielectric and gap capacitance.

The power was analyzed following the original work of Manley, who has utilized voltage–charge Lissajous figures to characterize the average consumed power through the discharge [32]. The charge–voltage characteristic plot was revealed in Fig. 5. The two values of effective discharge capacitance are indicated by obtaining of two distinct slopes of the Q–V plot. The DBD power formula was shown in Eq. (4), where is the total power P related to the operating frequency f, the peak voltage V_{max} and the minimum discharge voltage V_{min} at which microdischarges are monitored in the discharge gap with the capacitances of the dielectric(s) (C_D) and the gas gap (C_g).

$$p = \frac{1}{T}\int_0^T v(t) \cdot i(t)dt \; ; \quad i(t) = \frac{dQ}{dt}$$

$$p = \frac{1}{T}\int_0^T v(t) \cdot dQ$$

(4)

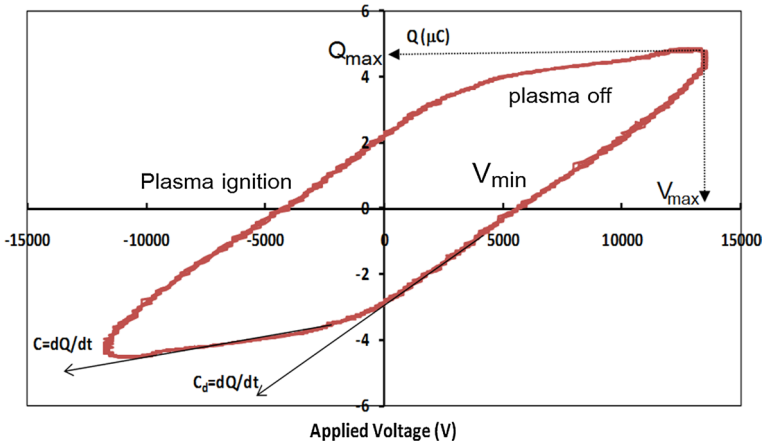$$\therefore P = 4fC_D^2\left(C_D + C_g\right)^{-1}V_{min}\left(V_{max} - V_{min}\right)$$

Fig. 5 Voltage–charge Lissajous figure at applied voltage 13 kV

The consumed power was determined to be 3 W at a voltage of 14 kV was applied.

Total Light Emission

In this work another independent method was used to confirm the formation of the filamentary discharge superimposing the homogeneous glow discharge modes. The total light emission intensity generated from plasma was detected with a fast photomultiplier. The response time of the photomultiplier was less than 1 ns which is short in comparison to the lifetime of the filaments in the discharge zone (higher than 10 ns). Figure 6 reveals the waveforms of the plasma discharge current (I) measured in milliampere and the total light emission intensity (LEI) following the discharge current presented in arbitrary unit.

It can be noticed that the emission intensity formed from filaments superimposed the uniform glow component that follow the discharge current behavior.

The formation of uniform glow discharge at atmospheric pressure may be attributed to different possibilities:
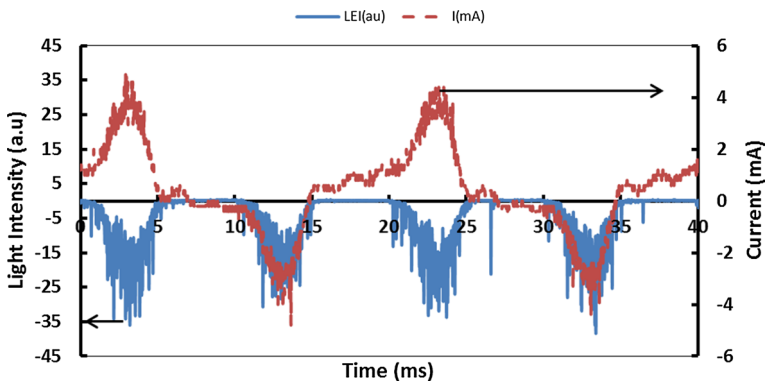

**Fig. 6** Total light emission and discharge current

1. The roughness of the dielectric surface forms many sharp edges which is expected to produce a high local electric field strength which is enough to cause ionization in the vicinity of the edges through the discharge volume leading to many streamers add together and forming the continuous glow discharge.
2. Emission of electrons from the dielectric surface due to a high electric field strength formed on the surface due to charge accumulation on the surface.
3. Some dielectric materials can trap appreciable amounts of charges uniformly on the surface. When the electric field changes its polarity, the charge carriers are expelled from the surface initiating a diffuse discharge development.

Contact Angle Measurements

The surface wettability of unmodified PVC membranes was derived from contact angle measurements of water drops set onto the PVC surface. High contact angles indicate hydrophobic, low contact angles display hydrophilic surface properties. The contact angle was measured for untreated, DBD plasma treatment in air, with additional AA grafting and finally after consumption of amine. As well known, oxygen plasma is a good source for introduction of polar oxygen-containing functional groups into the surfaces of the PVC membrane, which was reflected by better wetting with water and corresponding lower contact angles.

The results showed that the water contact angle (WCA) decreased from 54° of the original PVC to 18° of the DBD plasma-treated and acryl acid grafted PVC membrane (PVC-g-AA). However, the plasma treated and AA-grafted sample (PVC-g-AA) as well as the PVC-g-AA samples with additional amination (PVC-g-AA—Amin) show similar low water contact angles. This hydrophilicity is an indication of incorporation of polar O-containing groups into the surface as it was detected using FTIR-ATR spectroscopy (see "Study of Chemical Composition of the Membranes by ATR-FTIR" section). Previous work and those of other authors had also confirmed a reduction of WCA after plasma deposition of a plasma-polymerized layer of acrylic acid onto various substrates [40, 41]. Figure 7 shows the results of WCA tests.

Fig. 7 Contact angles of modified PVC compared to the untreated sample
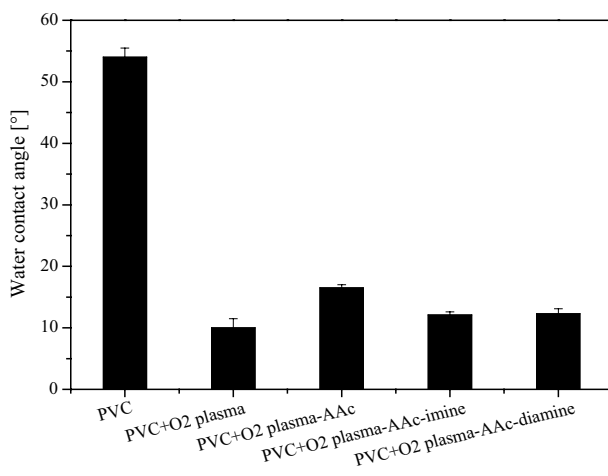
A tentative scheme of probable chemical reactions leading to the outstanding decrease of water contact angle is presented as follows ($\equiv$C = polymer surface):

1. After formation of C radicals ($\equiv$C$^{\cdot}$)
2. Molecular oxygen reacts with such radicals and forms peroxy groups ($\equiv$C$^{\cdot}$ + $^{\cdot}$O–O$^{\cdot}$ → $\equiv$C–O–O$^{\cdot}$). In a second step,
3. hydrogen abstraction from adjacent polymer molecules takes place ($\equiv$C–O–O$^{\cdot}$ + $\equiv$CH → $\equiv$C–O–OH + $\equiv$C$^{\cdot}$). An auto-oxidation process is now initiated. Then, the formed
4. hydroperoxide decomposes by plasma irradiation or plasma bombardment preferably to alkoxy and hydroxyl radicals ($\equiv$C–O–OH + hν → $\equiv$C–O$^{\cdot}$ + $^{\cdot}$OH). Now, the
5. alkoxy radicals can initiate the graft polymerization of acrylic acid ($\equiv$C–O$^{\cdot}$ + CH$_2$ = CH(COOH) → $\equiv$C–O–CH$_2$–CH(COOH)$^{\cdot}$ → further chain growth with new AA monomer molecules).

As discussed before, exposure to O$_2$ plasma is a good way to introduce polar O-functional groups such as OH, epoxy, C–O–C, >C=O, CHO, COOH, COOR etc. In addition, many radicals were generated but immediately consumed by molecular oxygen. The formed peroxy radicals then undergo the before described peroxy route. Therefore, two ways were possible to make hydrophilic the PVC surface by exposure to DBD discharge, firstly, the introduction of polar O and N containing groups and, secondly, additional post-plasma wet-chemical graft polymerization of acrylic acid with its strong polar carboxylic groups. Such post-plasma radical-initiated graft-copolymerization is a chain growth reaction which produces regularly structured covalently grafted poly(acrylic acid) [42]. Thus, a covalent bonding of the growing PAA chain to the PVC substrate is expected [43]. Such covalent grafting can be confirmed by the stability of grafted films towards solvent extraction.

Secondly, plasma-introduced O-functional groups can interact with the COOH groups of the grafted PAA molecules. Thus, PAA molecules which are not covalently bonded to the PVC substrate are also strongly adhered by such ionic or dipole–dipole interactions. In this way, homopolymers generated by radical transfer are also strongly bonded and can also withdraw solvent extraction. In plasma, there is a further possibility the well-known possibility of self-condensation of acrylic acid to esters, which is associated with loss in polarity.

Plasma-introduced OH groups can react with COOH groups of acrylic acid to ester groups. However, such reaction is not very probable. Such esterification needs a water absorbing additive to shift the reaction balance in favor of esterification.

It is worth to be mentioned the hydrophilicity plays a key role in adhesion, drug delivery, fuel cells, composite formation or polymer-complexes and bacteria behavior. Moreover, the results revealed that the WCA was strongly decreased (Fig. 7). Additionally, the wettability of the membranes was improved, however marginally, by the amination of COOH groups with polyethyleneimine or ethylenediamine.

Study of Chemical Composition of the Membranes by ATR-FTIR

The ATR-FTIR spectroscopy was utilized to study the chemical structure of the pure and modified PVC membranes. The ATR-FTIR spectra of unmodified PVC, PVC-g-PAA, and PVC-g-PAA–PEI (aminated with polyethyleneimine) samples are displayed in Fig. 8. The spectra of grafted samples differ from that of the blank PVC membrane. The spectrum
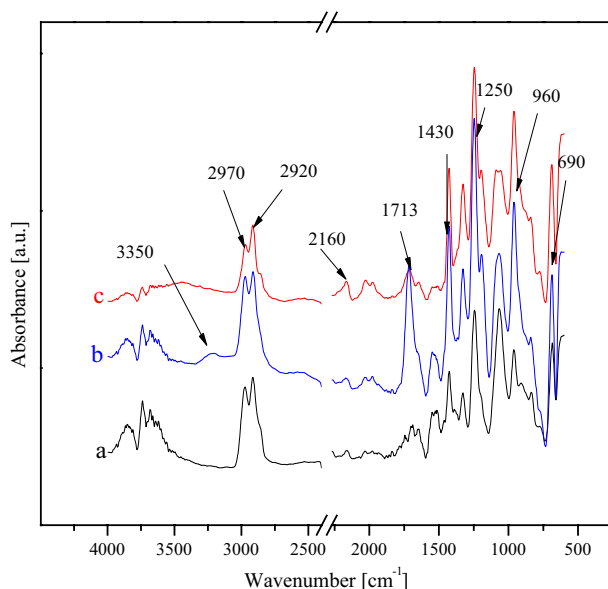
Fig. 8 FTIR-ATR spectra for (a) PVC as blank, (b) PVC-g-PAA, and (c) PVC-g-PAA–PEI

of PVC-g-PAA shows the characteristic peak for COOH groups at $\nu = 1713$ cm^{-1} (see also Table 1). A broader band covering a spectral range from 3000 to 2500 cm^{-1} reflects H-bonding interactions of COOH groups [44].

Fahmy and Schönhals [40] have been discussed that PAA components can be easily identified by νO–H in the range of 3200–3600 cm^{-1} corresponding to the O–H stretching mode and by its carbonyl vibration νC=O at ca. 1710 cm^{-1}. Additionally, the peak that was observed at 2920–2910 cm^{-1} could be identified as symmetric stretching vibrations of CH$_2$ and that of 2850–2840 cm^{-1} also. The observed absorption at 1430 and 840 cm^{-1} has been assigned to the δCH$_2$ and ωCH [45, 46].

As was presented in Fig. 8, a very strong band at 1713 cm^{-1} represents νC=O corresponding to the formation of a grafted PAA film. The regions of 1450–1400 cm^{-1} and 960–910 cm^{-1} are corresponding to the O–H in-plane and out-of-plane deformations, respectively. Although, the signal at 1450 cm^{-1} originates from the C–H bending vibration coupled with that of O–H bending [45]. Therefore, the IR spectra, depicted in Fig. 8, confirm the chemical modification of the membrane treated by oxygen plasma and grafted with PAA. Nevertheless, the C=O peak is shifted to 1740 cm^{-1} after amination with diamine. This shift may be referred to the amide formation [48, 49]. The found spectral features in the range of $\nu = 2160$ cm^{-1} represents the C≡N stretch, however, this is improbable. Amine hydrochloride formation is much more probable, and it corresponds very well with the before mentioned expectation of the existence of physically or hydrogen bonded PAA homopolymers [50].

Stability in Water

The stability of the PVC-g-AA membrane in water is very important with regard to biomedical or a fuel cells application, therefore, the solubility of the grafted films in water was

Table 1 Representation of the assignment of typical peaks in the IR spectra [45–47]

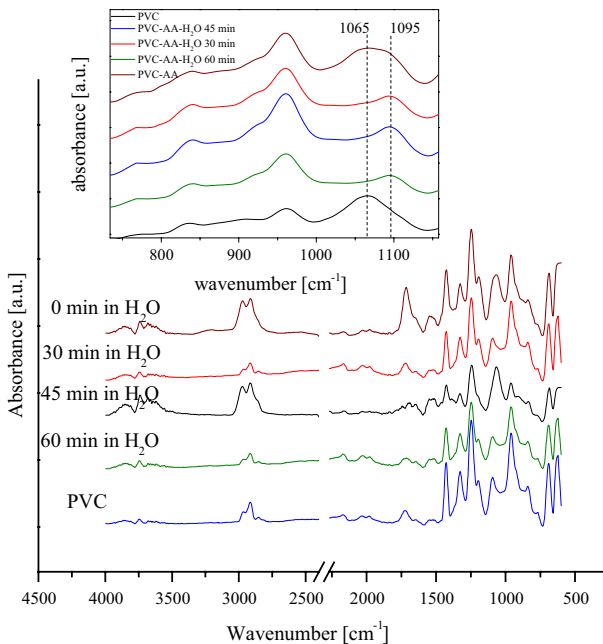| Material	Wavenumber (cm^{-1})	Vibration assignment
PVC	2970	νCH
	2920	ν^{ss}CH$_2$
	2870	νCH
	2850	ν^sCH$_2$
	1430	δCH$_2$
	1330	δCH $+ \tau$CH$_2$
	1250	δCH
	1198	νC–C
	1095	νC–C
	690, 640, 613	νC–Cl
PVC-O$_2$ plasma-PAA (PVC–PAA)	3200–3600	νO–H
	1710	νC=O
	1451	δCH$_2 + \delta$O–H$_{in\ plane}$
	1402	δOH $+ \nu$C–O
	1250	δCH and νC–O $+ \delta$OH
	960	δO–H
PVC–PAA-amination with polyethyleneimine	3300–3500	ν^{as} and ν^s N–H
	2160	νCN
	1740	ν^{as} C=O amide I
	1655	δN–M
	1064	$\nu_{C–N}$ (chain not amide) or δ_{CH3}

Fig. 9 FTIR-ATR spectra of PVC-O$_2$ plasma-AA with dipping in dist. water for 30, 45 and 60 min compared to the pure PVC membrane as blank. The inset reveals spectra from 1150 to 750 cm^{-1} as example

investigated. Figure 9 reveals the spectra of the original, modified and grafted PVC membranes before and after washing in water. A definite amount of PAA layer was dissolved from the grafted films after water exposing with increasing the washing time, indicated by the loss in transmittance at $\nu = 1713$ cm^{-1} ($\nu_{C=O}$). It can be interpreted by removing of some non-bonded homopolymer with low molecular weight.

Other oxygen specific signals such as δO–H and νC–O at wavenumbers of 960 and 1095 cm^{-1} remain unchanged as shown in the inset of Fig. 9 [51]. These results suggest that the modified PVC membrane was successfully grafted by a thin film of PAA although partially PAA homopolymers were also produced.

Surface Morphology

Figure 10 displays microscopic images (SEM) which show the surface morphology of blank PVC, PVC-g-PAA and PVC-g-PAA–PEI (PEI—polyethyleneimine). In the aminated membranes phase separation was not observed. The smooth surface morphology and glossy-like structure of the PVC-g-PAA membrane (Fig. 10) refers the homogeneity and the good compatibility between PVC and PAA.

Investigation of Thermal Stability of the Modified PVC Membrane by Thermogravimetry (TGA)

The percentage of weight loss as function of original PVC and PVC-g-PAA membranes is presented in Fig. 11. The weight loss of modified membranes is lower than that of
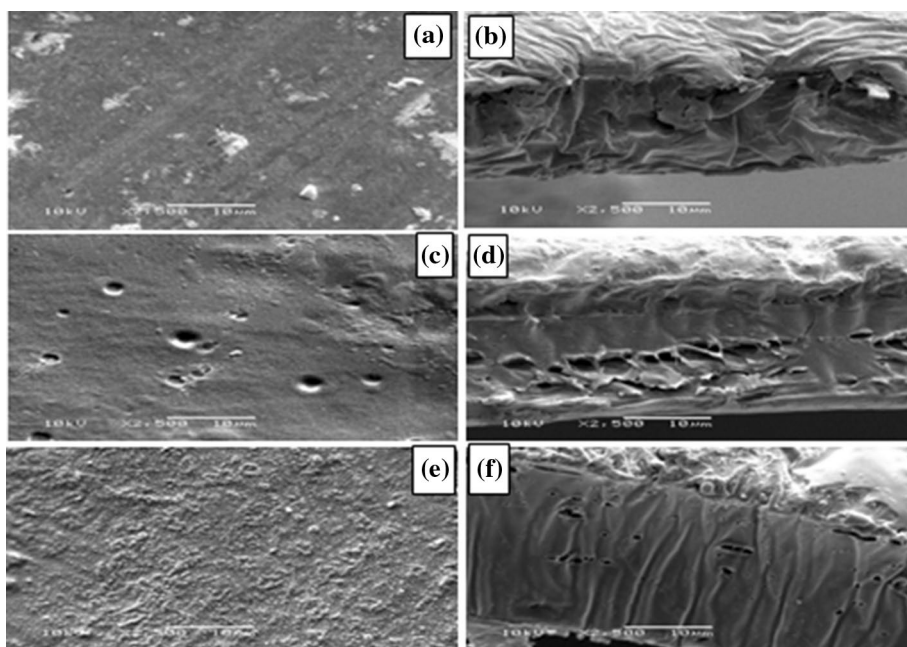

Fig. 10 Scanning electron micrographs of unmodified **a** PVC, **c** PVC-g-PAA, **e** PVC-g-PAA–PEI on the left side while the cross-sections of each sample are shown on the right side, respectively
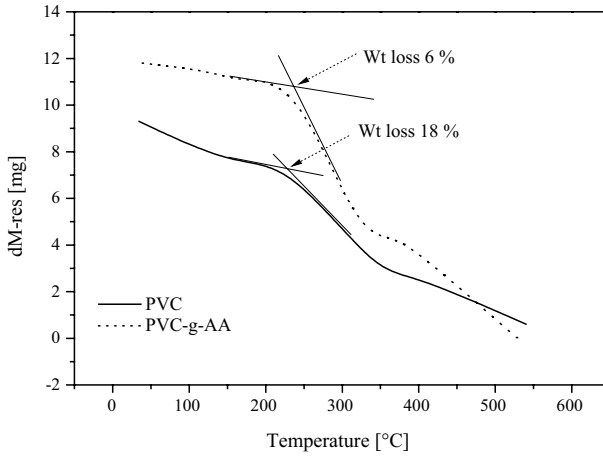
Fig. 11 TGA experiments on PVC-g-PAA in comparison to unmodified PVC

unmodified PVC indicating a thermally stable grafting of membrane. This thermal stability is high enough for its application in the direct methanol fuel cell (DMFC) [52] since the thermal decomposition of the grafted membrane does not start below 250 °C.

For all membranes, a small transition around 100 °C is observed, which corresponds to weight loss of absorbed water. The transition at about 380 °C is assigned to the beginning of chain scissions. The weight loss to the threshold of 250 °C was much lower for the PVC-g-PAA (6%) than for the original PVC (18%).

Ion Exchange Capacity Measurements (IEC)

Figure 12 presents the IEC values of the various processes to modify PVC membranes.

The IEC value of unmodified PVC is very low as expected because of the low level of charges present in such polymer membranes. After modification by exposure to the DBD atmospheric-pressure plasma and subsequent grafting with PAA the IEC value

Fig. 12 The change of IEC values in PVC-g-PAA–PEI at wide range of time for amination compared to PVC-g-PAA and untreated PVC
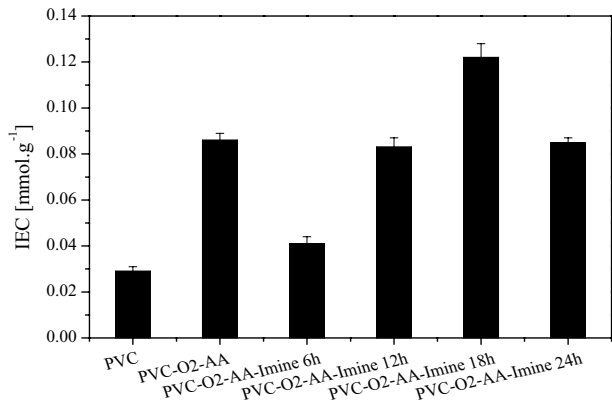
was increased. Additional amination with PEI shows a slightly lower IEC value when the reaction time for amination was shorter than 6 h. It should be remembered that the carboxylic groups of PAA should be consumed by the PEI reacting to amide groups. Therefore, the IEC values decreased after amination process for 6 h. However, a clear trend is noted for prolonged amination reaction. The IEC value of PVC-g-PAA–PEI after 12 h amination is close to that of the PVC-g-PAA. It means that PVC-g-PAA membranes without subsequent amination are also suitable as electrolyte membranes. Thus, an additional reaction process can be eliminated. Nevertheless, prolonged amination of 18 h further increases the IEC value (Fig. 12). In summary, with increasing the polarity of membrane surfaces, the IEC values were increased also considering the risen water content in the polymer membrane, therefore, the water uptake measurement was recommended for confirmation.

Solvent Uptake

The study of swelling ability of polymer membranes was previously reported [53]. The adsorption ability or more colloquially swelling degree (uptake %) of PVC-g-PAA–PEI, compared to the untreated PVC membrane is shown in Fig. 13. The swelling measurements performed with deionized water, methanol and ethanol at room temperature.

The treatment of PVC membranes influenced the degree of swelling strongly. The resultant swelling data refer that the grafted PAA acts as an electrolyte and therefore, the water uptake of the PVC-g-PAA was significantly increased and that of PVC-g-PAA–PEI was further increased. However, the adsorption ability/swelling degree of the modified membrane depends on the density of polar groups (COOH, NH_x, –CO–NH–) at the membrane surface and the polarity of solvent ($H_2O > CH_3OH > C_2H_5OH$), thus the polar solvent molecule was attracted by the membrane surface with many polar groups or the more aliphatic solvent was repelled. Further, the maximum uptake of water was achieved with the aminated PVC-g-PAA–PEI membrane. The PAA grafted membrane (PVC-g-PAA) adsorbs alcohols preferentially [54].

Fig. 13 Water, methanol and ethanol uptake (%) of PVC-g-PAA–PEI within 12 h compared to the untreated PVC membrane
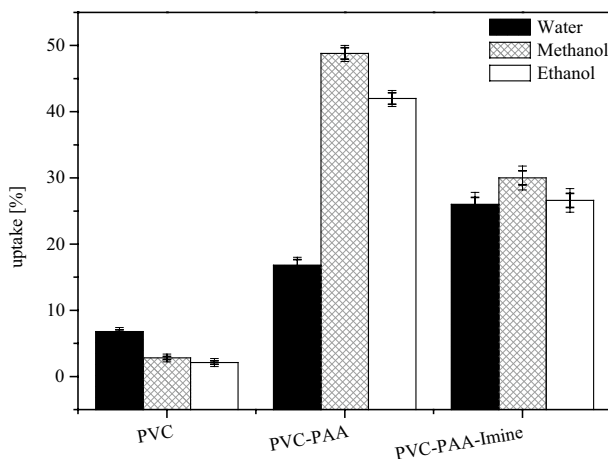
Summary

Acrylic acid was successfully graft-polymerized onto PVC membranes using a preceding exposure to the atmospheric-pressure DBD plasma in air/O_2 gas. The thus modified membrane fulfilled the preconditions for use as electrolyte membrane if subsequently to the plasma modification a wet-chemical grafting from of poly(acrylic acid) has taken place. Thus, a strong polar membrane surface was generated equipped with carboxylic groups. Further reacting of carboxylic groups with amino groups of polyethyleneimeine has produced an insignificantly stronger polarity.

The produced increased polarity of the PVC surface was quantified by measurements of water contact angles and FTIR-ATR spectroscopy. Additionally, the weight loss of all modified PVC membranes was much lesser than that of original PVC. Such modified PVC-O_2 plasma-AA membrane can be now applied as an electrolyte membrane.

References

1. Kamoun EA, Youssef ME, Abu-Saied MA, Fahmy A, Khalil HF, Abdelhai F (2015) Ion conducting nanocomposite membranes based on PVA-HAHAP for fuel cell application: iI. Effect of modifier agent of PVA on membrane properties. Int J Electrochem Sci 10:6627
2. Venkatesan PN, Dharmalingam S (2017) Characterization and performance study of phase inversed Sulfonated Poly Ether Ether Ketone–Silico tungstic composite membrane as an electrolyte for microbial fuel cell applications. Renew Energy 102:77
3. Tseng CY, Ye YS, Cheng MY, Kao KY, Shen W-C, Rick J, Chen J-C, Wang B-J (2011) Sulfonated polyimide proton exchange membranes with graphene oxide show improved proton conductivity, methanol crossover impedance, and mechanical properties. Adv Energy Mater 1:1220
4. Fu YZ, Manthiram A, Guiver MD (2007) Acid–base blend membranes based on 2-amino-benzimidazole and sulfonated poly(ether ether ketone) for direct methanol fuel cells. Electrochem Commun 9:905
5. Jiang Z, Zhao X, Fu Y, Manthiram A (2012) Composite membranes based on sulfonated poly(ether ether ketone) and SDBS-adsorbed graphene oxide for direct methanol fuel cells. J Mater Chem 22:24862
6. Wang J, Liao J, Yang L, Zhang S, Huang X, Ji J (2012) Highly compatible acid–base blend membranes based on sulfonated poly(ether ether ketone) and poly (ether ether ketone-alt-benzimidazole) for fuel cells application. J Membr Sci 415–416:644
7. Jiang Z, Jiang Z-J (2014) Plasma techniques for the fabrication of polymer electrolyte membranes for fuel cells. J Membr Sci 456:85
8. Follain N, Roualdes S, Marais S, Frugier J, Reinholdt M, Durand J (2012) Water transport properties of plasma-modified commercial anion-exchange membrane for solid alkaline fuel cells. J Phys Chem C 116:8510
9. Reinholdt M, Ilie A, Roualdès S, Frugier J, Schieda M, Coutanceau C, Martemianov C, Flaud V, Beche E, Durand J (2012) Plasma membranes modified by plasma treatment or deposition as solid electrolytes for potential application in solid alkaline fuel cells. Membranes 2:529
10. Navarro A, delRío C, Acosta JL (2009) Pore-filling electrolyte membranes based on plasma-activated microporous PE matrices and sulfonated hydrogenated styrene butadiene block copolymer (SHSBS) Single cell test and impedance spectroscopy in symmetrical mode. Solid State Ionics 180:1505
11. Bébin P, Caravanier M, Galiano H (2006) Nafions/clay-SO_3H membrane for proton exchange membrane fuel cell application. J Membr Sci 278:35
12. Unger WES, Swaraj S, Oran U (2006) Radio frequency (r.f.) plasma-deposited polymer films: influence of external plasma parameters as viewed by comprehensive in situ surface chemical analysis by XAS, XPS and ToF-SIMS. Surf Interface Anal 38:522
13. Scheltjens G, Ponte GD, Paulussen S, de Graeve I, Terryn H, Reniers F, van Asche G, van Mele B (2015) Thermal properties of plasma deposited methyl methacrylate films in an atmospheric DBD reactor. Plasma Process Polym 12:260

14. Fridman A (2008) Plasma chemistry. Cambridge University Press, New York
15. Pelaz B, del Pino P, Maffre P, Hartmann R, Gallego M, Rivera-Fernández S, de la Fuente JM, Nienhaus GU, Parak WJ (2015) Surface functionalization of nanoparticles with polyethylene glycol: effects on protein adsorption and cellular uptake. ACS Nano 9:6996
16. Lei S, Wang X, Li B, Kang J, He Y, George A, Ge L, Gong Y, Dong P, Jin Z, Brunetto G, Chen W, Lin Z-T, Baines R, Galvao DS, Lou J, Barrera E, Banerjee K, Vajtai R, Ajayan P (2016) Surface functionalization of two-dimensional metal chalcogenides by Lewis acid−base chemistry. Nat Nanotechnol 11:465
17. Biederman H, Slavínská D (2000) Plasma polymer films and their future prospects. Surf Coat Technol 125:371
18. De Vietro N, Belforte L, Lambertini VG, Fracassi F (2014) Low-pressure plasma modified polycarbonate: a transparent, low reflective and scratch resistant material for automotive applications appl. Surf Sci 307:698
19. Nisol B, Batan A, Dabeux F, Kakaroglou A, De Graeve I, Van Assche G, Van Mele B, Terryn H, Reniers F (2013) Surface characterization of atmospheric pressure plasma-deposited allyl methacrylate and acrylic acid based coatings. Plasma Process Polym 10:564
20. Batan A, Brusciotti F, De Graeve I, Vereecken J, Wenkin M, Piens M, Pireaux JJ, Reniers F, Terryn H (2010) Comparison between wet deposition and plasma deposition of silane coatings on aluminium. Prog Org Coat 69:126
21. Vilani C, Weibel DE, Zamora RRM, Habert AC, Achete CA (2007) Study of the influence of the acrylic acid plasma parameters on silicon and polyurethane substrates using XPS and AFM. Appl Surf Sci 254:131
22. Weibel DE, Vilani C, Habert AC, Achete CA (2007) Surface modification of polyurethane membranes using low-powered gas plasmas. Influence on the pervaporation processes. J Membr Sci 293:124
23. Solouk A, Solati MH, Najarian S, Mirzadeh H, Seifalian AM (2011) Optimization of acrylic acid grafting onto POSS-PCU nanocomposite using response surface methodology. Iran Polym J 20:91
24. Fahmy A, Friedrich J (2013) Degradation behavior of thin polystyrene films under exposure to Ar-plasma and its emitted radiation. J Adhes Sci Technol 27:324
25. Desmet T, Morent R, Geyter N, Leys C (2009) Nonthermal plasma technology as a versatile strategy for polymeric biomaterials surface modification: a review. Biomacromol 10:2351
26. Keshvari H, Mirzadeh H, Mansoori P (2008) Collagen immobilization onto acrylic acid laser-grafted silicone for using as artificial skin: in vitro. Iran Polym J 17:171
27. Perni S, Kong MG, Prokopovich P (2012) Cold atmospheric pressure gas plasma enhances the wear performance of ultra-high molecular weight polyethylene. Acta Biomater 8:1357
28. D'Sa RA, Burke GA, Meenan BJ (2010) Protein adhesion and cell response on atmospheric pressure dielectric barrier discharge-modified polymer surfaces. Acta Biomater 6:2609
29. Shao T, Zhang C, Long K, Zhang D, Wang J, Yan P, Zhou Y (2010) Surface modification of polyimide films using unipolar nanosecond-pulse DBD in atmospheric air. Appl Surf Sci 256(12):3888
30. Morent R, De Geyter N, van Vlierberghe S (2011) Influence of operating parameters on plasma polymerization of acrylic acid in a mesh-to-plate dielectric barrier discharge. Prog Org Coat 70:336
31. Sardella E, Favia P, Dilonardo E, Petroni L, d´Agostino R (2007) PE-CVD of Acid/base coatings from acrylic acid and allylamine vapours. Plasma Process Polym 4:S781
32. Manley TC (1943) The electric characteristics of the ozonator discharge. Trans Electrochem Soc 84(1):83
33. Kogelschatz U (2002) Dielectric-barrier discharges: their history, discharge physics and industrial applications. IEEE Trans Plasma Sci 30(4):1400
34. Zainoodin AM, Kamarudin SK, Masdar MS, Daud WRW, Mohamad AB, Sahari J (2014) High power direct methanol fuel cell with a porous carbon nanofiber anode layer. J Appl Energy 113:946
35. Yang C, Chiu S, Kuo S (2011) Preparation of poly (vinyl alcohol)/montmorillonite/poly (styrene sulfonic acid) composite membranes for hydrogen–oxygen polymer electrolyte fuel cells. J Curr Appl Phys 11:229
36. Hasan M, Narayan A, Lee M (2015) Enhanced thermo-optical performance and high BET surface area of graphene PVC nanocomposite fibers prepared by simple facile deposition technique: N_2 adsorption study. J Ind Eng Chem 21:828
37. Elamathi S (2010) Synthesis and characterization of polymer electrolyte membranes for fuel cell application, chapter two. Ph.D., Anna University, Chennai-Madras, India
38. Abu-Saied M, Fontananova E, Drioli E, Mohi Eldin MS (2013) Sulphonated poly(glycidyl methacrylate) grafted cellophane membranes: novel application inpolyelectrolyte membrane fuel cell (PEMFC). J Polym Res 20(7):1

39. Brandenburg R (2017) Dielectric barrier discharges: progress on plasma sources and on the under-standing of regimes and single filaments. Plasma Sources Sci Technol 26:053001
40. Fahmy A, Schönhals A (2016) Reaction of CO_2 gas with (radicals in) plasma polymerized acrylic acid (and formation of COOH-rich polymer layers). Plasma Process Polym 13:499
41. Villegas M, Romero AI, Parentis ML (2016) Acrylic acid plasma polymerized poly(3-hydroxybu-tyrate) membranes formethanol/MTBE separation by pervaporation. Chem Eng Res Des 109:234
42. Fahmy A, Debarnot D, Friedrich J (2015) Influence of water addition on the structure of plasma-deposited allyl alcohol polymer films. J Adhes Sci Technol 29(10):965
43. Fahmy A, Friedrich J, Poncin-Epaillard F, Debarnot D (2016) Plasma polymerized allyl alcohol/O_2 thin films embedded with silver nanoparticles. Thin Solid Films 616:339
44. Rezaei F, Shokri B, Sharifian M (2016) Atmospheric-pressure DBD plasma-assisted surface modifica-tion of polymethyl methacrylate: a study on cell growth/proliferation and antibacterial properties. Appl Surf Sci 360:641
45. Merche D, Poleunis C, Bertrand P (2009) Synthesis of polystyrene thin films by means of an atmos-pheric-pressure plasma torch and a dielectric barrier discharge. IEEE Trans Plasma Sci 37(6):951
46. Del Fanti NA (2008) Infrared spectroscopy of polymer. Thermo Fisher Scientific Inc., Waltham
47. Fahmy A, Eisa WH, Yosef M, Hassan A (2016) Ultra-thin films of poly(acrylic acid)/silver nanocom-posite coatings for antimicrobial applications. J Spectrosc 2016:1
48. Mahfoudh A, Barbeau J, Moisan M, Leduc A, Seguin J (2010) Biocidal action of ozone-treated poly-styrene surfaces on vegetative and sporulated bacteria. Appl Surf Sci 256(10):3063
49. Fahmy A, El-Nasser KS, Ali IO, Salama TM, Altmann K, Friedrich JF (2017) Tuning of adhesion of silver nanoparticles onto zeolite ZSM-5 using electrospray ionization (ESI) encapsulation with poly (acrylic acid). J Adhes Sci Technol 31(24):2641
50. Fahmy A, Mohamed TA, Friedrich JF (2018) XPS and IR studies of plasma polymers layer deposited from allylamine with addition of ammonia. Appl Surf Sci 458:1006
51. Morent R, De Geyter N, Trentesaux M, Gengembre L, Dubruel P, Leys C, Payen E (2010) Stability study of polyacrylic acid films plasma-polymerized on polypropylene substrates at medium pressure. Appl Surf Sci 257:372
52. Edwards HGM, Brown DR, Dale JA, Plant S (2000) Raman spectroscopy of sulphonated polystyrene resins. J Vib Spectrosc 24:213
53. Mohanapriya S, Bhat SD, Sahu AK, Manokaran A, Vijayakumar R, Pitchumani S, Sridhar P, Shukla AK (2010) Sodium-alginate-based proton-exchange membranes as electrolytes for DMFCs. Energy Environ Sci 3:1746
54. Maiti J, Kakati N, Lee SH, Jee SH, Viswanathan B, Yoon YS (2012) Where do poly(vinyl alcohol) based membranes stand in relation to Nafion® for direct methanol fuel cell applications? J Power Sources 216:48

Springer